BIFACIAL PV SYSTEMS AT HIGH LATITUDE: MODELING AND VALIDATION WITH MONITORING DATA

Hugo E Huerta[1], Samuli Ranta[1], Shuo Wang[1], Aleksi Heinonen[1], Sami Jouttijärvi[2], Anton Driesse[3], Kati Miettunen[2]
1. New Energy Research Group, Turku University of Applied Sciences, Joukahaisenkatu 7, 20520 Turku
2. Department of Mechanical and Materials Engineering, University of Turku, Vesilinnantie 5, 20500 Turku, Finland
3. PV Performance Labs, Emmy-Noether-Str. 2, Freiburg, Germany
Corresponding author: Hugo Huerta, hugo.huertamedina@turkuamk.fi

ABSTRACT: In this paper, we model and evaluate the performance of two different Bifacial Photovoltaic implementations at high latitude locations with latitudes close to 60° N, consisting of a set of seaside PV canopies with 100 kWp power and a roof-mounted PV system with 140 kWp power. The modelling is done by using the backward ray-tracing technique in combination with detailed 3D models to achieve a more accurate evaluation of the rear-side irradiance and energy yield prediction. An improved irradiance sampling method was developed to simulate an accurate irradiance map on each cell of the modules with high-speed asynchronous execution. The detailed irradiance power output of the canopy system was simulated over one year and compared with monitored data for an analysis of energy gain and loss. Results show that 7% of the total energy comes from the rear irradiance, in which 1% of the total energy is from the enhancement of snow. However, snow coverage on the front side could cause a loss of 2.8% of the total energy, which indicates that an appropriate snow clean-up measure might be important to further optimize the yield of PV systems in high latitude regions. The methodology was implemented preliminarily for the second configuration, roof-mounted PV to prove its replicability. Preliminary results show only 2% of the energy is produced by the rear side. The modelling methodology was proven to be reliable and useful when evaluating different bifacial PV configurations.

Keywords: Bifacial, Ray-Tracing, High-Latitudes, Modelling.

1 INTRODUCTION

Bifacial Photovoltaic (BPV) modules have emerged as a promising technology in the field of solar energy generation, offering the potential to significantly enhance the efficiency and energy yield of solar installations. Unlike conventional PV modules, which capture sunlight only from their front surfaces, bifacial modules can also harvest energy from the rear side by capturing the light reflected off by the nearby surfaces such as the ground, buildings, and other objects. This unique characteristic has increased the interest in bifacial technology, particularly in applications where maximizing energy production from limited space is crucial, such as installations on flat roofs and solar farms. However, the accurate modeling and simulation of bifacial PV modules present substantial challenges, primarily from the difficulty in accurately estimating the incident irradiance at the rear side of the modules. The incident irradiance, or the amount of sunlight received by the rear surface, plays a critical role in determining the overall performance and energy generation of bifacial modules. Consequently, limitations in accurately characterizing this parameter can significantly impact the reliability of predictive models and the design of efficient bifacial solar systems.

Within the PV community, two primary methods have been used [1], namely geometric factors and ray-tracing methods. The View factor model [2] employs a simplified approach to compute bifacial irradiance. It utilizes view factors for 2D geometric representations of PV arrays. This method is particularly advantageous for estimating the energy production of big PV arrays due to its computational efficiency, completing annual hourly simulations in just a few seconds. The main characteristic in this method is that it considers infinite PV rows, in consequence ignoring the edge effects as well as the lack of light behavior physics behind the model**.** Ray-tracing methods [3] simulate the paths of individual rays of sunlight as they interact with the module and its surroundings. By tracing the rays through a three-dimensional representation of the PV module, ground, and nearby objects, ray-tracing models can provide a more detailed and accurate estimation of rear-side irradiance. Nonetheless, they require substantial computational resources and can be complex to implement.

In this study, we model and validate results with a pilot site by implementing the ray-tracing method. By using Radiance [4] software which excels in simulating the behavior of light in complex environments to estimate how light interacts with surfaces, materials, and objects when considering factors such as reflections, refractions, and shadows. Additionally, we integrated the use of Bifacial-Radiance [5] tool which is a software extension built upon the Radiance platform and is designed to facilitate the modeling and analysis of bifacial PV systems. These tools are combined to model and evaluate the performance of two different Bifacial PV implementations at high latitude locations, where the seasonal changes, long days during the summer and short and dark days with/without snow during the winter play an important role in the solar energy production. To complete this study, two different BPV system configurations in different locations are considered. The first system, used for validation, hereafter referred to as the 'Canopy-PV array,' consists of a 100 kWp bifacial system integrated into seaside canopies. This system, located in Naantali, Finland, has been in operation since June 2022 and includes six canopies, each equipped with a varying number of bifacial modules (36, 48, or 60) rated at 350 Wp. The modules are tilted at an angle of 15°, with the bottom edge of the modules positioned 3.5 meters above the ground. Different materials integrate the surfaces under the Canopies like gravel, wood and even water, all having different albedo conditions which range from 30 – 55%. The canopies' roof orientations vary slightly (+-10°) from the South.

The second system, modeled for replicability and with preliminary results, hereafter referred to as the 'Flat-Roof

PV array', consists of a 140 kWp bifacial system scheduled for installation in autumn 2023 on the roof of a new student housing unit in Turku, Finland. These bifacial modules, rated at 360 Wp, were designed and manufactured by a local company. They will be installed on the building's roof with a tilt angle of 15° and oriented towards the South; The building's roof is covered by membrane with an albedo value around 14%.

2 METHODOLOGY

2.1 Monitoring data collection

Data collection to validate the modeling of the Canopy-PV array commenced in mid-summer 2022 by monitoring DC voltage and current for two PV strings with a 1-second time resolution. On-site meteorological data is gathered using a ventilated pyranometer to measure global tilt irradiance (GTI) and a weather transmitter to record air temperature, wind speed, and other relevant variables. Additionally, six reference cells were strategically positioned, 5 of them facing downward along the rear-side of the canopy enabling the measurement of rear-side plane of array (POA); The sixth cell was placed at the same modules tilt angle for measuring POA irradiance. The study collected irradiance and power output data from the Canopy-PV system for a one-year period, spanning from July 2nd, 2022, to July 1st, 2023. Throughout this timeframe, a total of 530 hours of monitoring data were unavailable due to blackouts or system updates. Thus, there were in total 8230 hours (343 days) of effective monitoring data that were available for validation and analysis. A comprehensive description of the monitoring system is shown in our previous work [6].

For the Flat-Roof PV array, the simulations utilized the same meteorological data from the Canopy-PV due to delays in the installation of the system.

2.2 System modelling

Both PV arrays underwent 3D modeling to create realistic representations of the buildings and mounting systems **Figure 1**. In the case of smaller BPV systems, such as those studied here, the inclusion of more details becomes essential. These details include accounting for mounting systems, understructures, and even the spacing between modules and cells. At this scale, the inhomogeneity of rear-side irradiance becomes more pronounced due to stronger edge effects leading to power mismatches among cells and modules at various positions.

To address this challenge, a complex and computationally intensive method for detailed irradiance mapping, known as reverse ray-tracing with Radiance, was employed. This method involves tracing a large number of photon paths using the Monte Carlo method and simulating object interference within the modeled system. It allows for optical simulations by incorporating properties such as albedo for various ground/roof conditions as well as specularity, and reflectance of the structures and mounting systems into the model.

This study focused primarily on three columns of PV modules (18 in total) from Canopy-PV, constituting a single string with 6.3 kWp. To evaluate the electrical properties of the PV modules, a two-diode model was employed. The model incorporated average values derived from flashing tests of 50 modules.

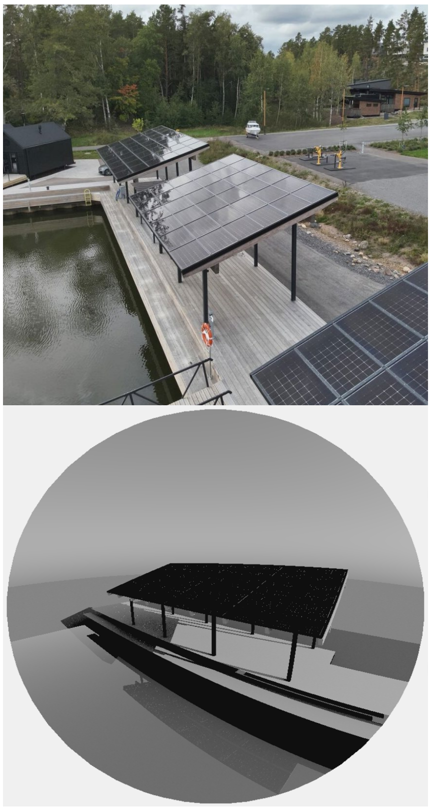

Canopy-PV array (top), 3D models rendering (bottom)

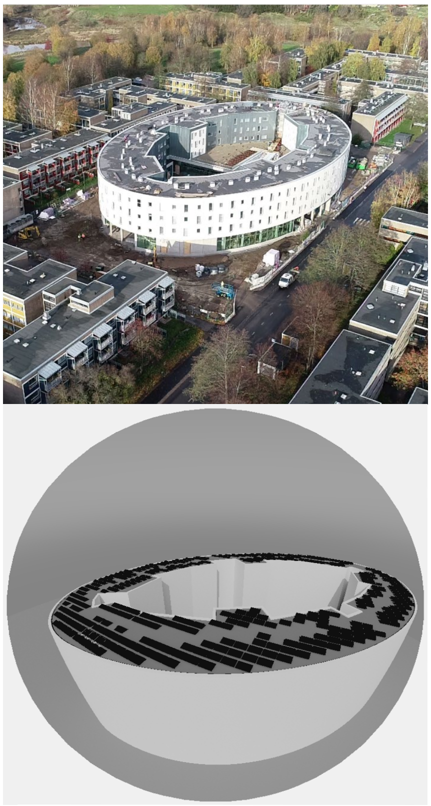

Flat-Roof PV- building (top), 3D model rendering (bottom)

Figure 1:PV systems under study: 3D models were built to cell-scale level and used in Radiance software for modelling rear-side irradiance. Rendering using acceleradRT [6]

10.4229/EUPVSEC2023/4BO.5.4

The initial model, as described in a previous work [6], underwent expansion to incorporate electrical calculations for the entire system. The integration of the SUNPOWER PVMismatch module enabled the computation of both power output and mismatch loss.

An enhanced sampling method was introduced to facilitate irradiance calculations for individual cells within the PV modules of interest in conjunction with a high-level interface method for asynchronously executing the simulations, resulting in a significant reduction in simulation time. Bifacial-Radiance tool in combination with the measured data and the detailed irradiance maps were used for the thermal and electrical modelling, resulting in the BPV output, the whole process is detailed in **Figure 2**.

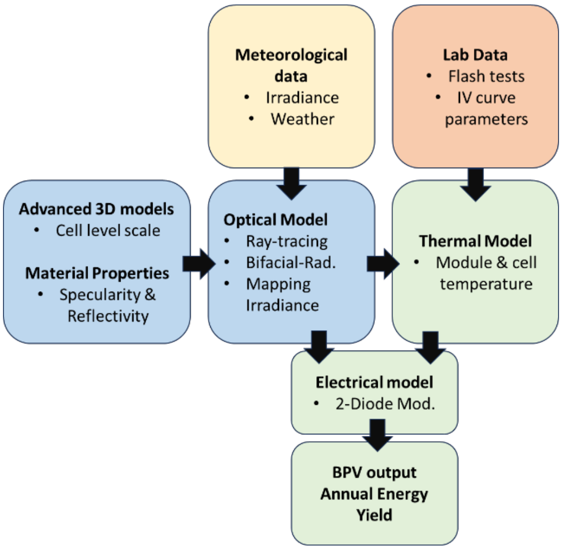

Figure 2: Framework used for modelling the performance of bifacial PV systems

To account for the influence of snow, which is critical in this region, snow depth data was obtained from the Finnish Meteorological Institute at Turku Artukainen station, located approximately 8 km from the Canopy-PV array system and 5 km from the Flat-roof PV array system. Timestamps with snow depth greater than zero were classified as "snow conditions". While acknowledging some variation between the weather station's snow condition data and the canopy system's location, this approach sufficed for distinguishing ground conditions with and without snow. The work as described is intended to establish a practical and accurate methodology using the ray-tracing technique for bifacial systems at high latitudes validating it with on-site measured data, tackling at the same time the previously mentioned challenges.

3 RESULTS

3.1 Canopy-PV

1. Model validation

a) Rear irradiance

The rear irradiance detected by the sensors was used to validate the albedo parameters. The reference albedo of ground objects in the model was optimized by the method as described in our last paper [7]. **Figure 3** shows the comparison between simulated and measured irradiance at five sensors on the backside and the average value over the five sensors for a sunny day in August 2022. In general, the simulations fit with the measured irradiance well, only with slight deviations for sensor 1 in the afternoon.

With the reference albedo, the detailed irradiance on both sides of modules were simulated by an improved sampling method. This method enables fast and accurate sampling on every cell on the module. **Figure** 4 illustrates the irradiance map of the whole canopy from the back side for a sunny day on 25 August. Note that the target string is the left three columns in the figure.

The hourly averaged bifacial gain of the target module string can be evaluated from the irradiance map and shown in **Figure** 5. Since the target string is in the eastern part of the system, in sunny days it gets more light on the backside in the morning, which results in higher bifacial gain up to over 30% during that period. With the Sun moving to south, the bifacial gain decreases to the lowest gain around 9% in the afternoon. In cloudy days like 21 and 24 August, the bifacial gain tends to be constant (around 13%) over the whole day.

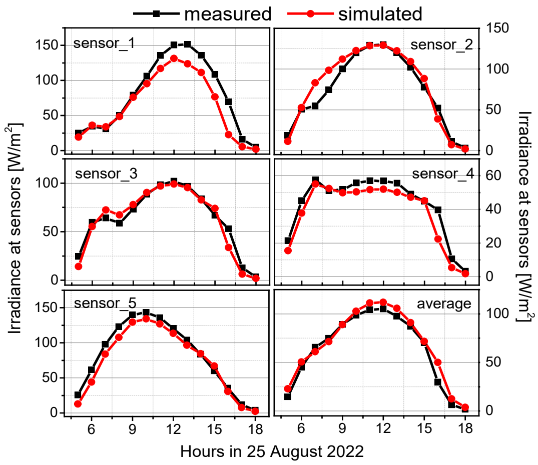

Figure 3: Measured and simulated hourly irradiance on back sensors and their average value over a sunny on 25 August 2022.

b) Power output and mismatch

The power output of the target string of the same week was simulated by the electrical model and shown in **Figure** 6. The sampled irradiance at each cell in the module was used to calculate the power with mismatch loss (P_{mm}), while the average irradiance was used to calculate the power output without mismatch (P_{ave}). The simulations show good coherence with the measured data, although with slight overestimation. The power simulated with mismatch is slightly lower than the power without mismatch, which is due to the mismatch loss. When the power is integrated over the sunny day on the 25th, the simulated power with mismatch is about 4% higher than the measured power. This difference may be partly due to possible losses that we lack in our model, such as PV module variation, soiling effect, wire connection loss, and MPPT loss.

The hourly mismatch loss of the same week is analyzed in detail in **Figure 7.** The mismatch loss (MM) is defined as:

$$MM = (P_{mm} - P_{ave})/P_{ave} \qquad (1)$$

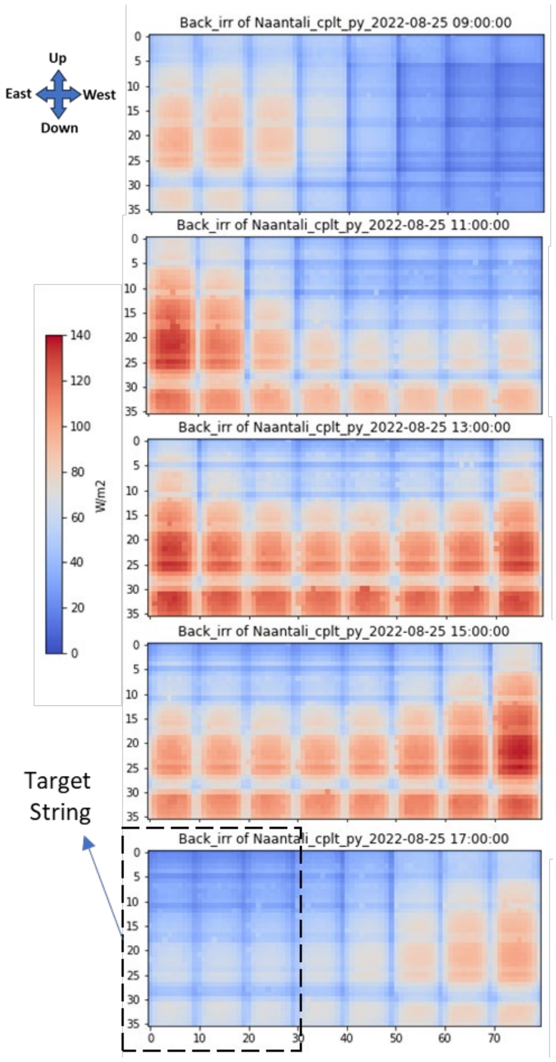

Figure 4: Rear irradiance mapof the system for a sunny day on 25 August 2022. The x- and y-axis indicate the number of cells. The perspective in the figure is from north to south. The three columns of modules in the eastern part were taken as the target string for detailed investigation.

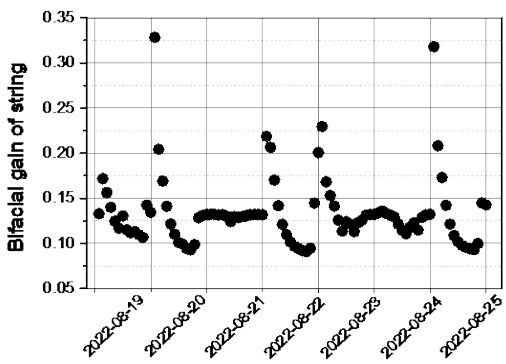

Figure 5: The calculated hourly bifacial gain of the target string in the week from 19 to 25 in August 2022

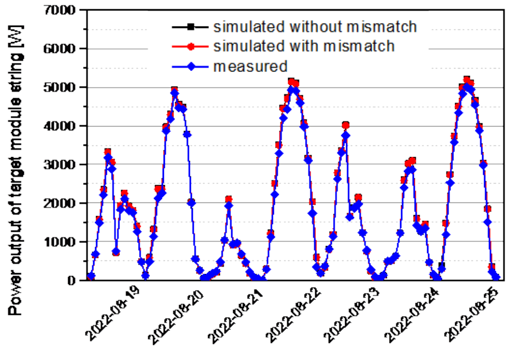

Figure 6: The simulated and measured hourly power output of the target string in one week in August 2022.

The mismatch loss is dependent on the time of the day, which is larger in the morning and late afternoon. The highest loss can be over -1%, while for most time in the day it is around -0.4%.

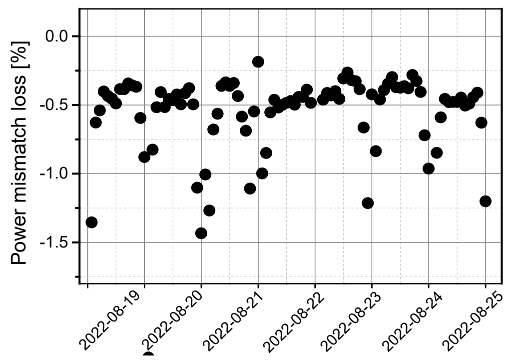

Figure 7: The hourly power mismatch loss of the target string in one week in August 2022.

2. Evaluation over the whole year

After validation and initial analysis of the model, simulations throughout the year were performed to understand the performance of the system and the energy losses. As the albedo of the ground can be dramatically changed by snow, the discussion was divided into two parts, the days with and without snow on the ground.

a) Days without snow

When comparing the simulated irradiance on the rear sensors with the measured data over a longer period, it was found that a single set of albedo parameters was insufficient to fit all the conditions well. The ground conditions keep changing over time, such as alterations in wood color (aging) and its differences in color between wet and dry conditions. As shown in **Figure 8**, the irradiance on rear sensors was aggregated into days, and the ratio of measured to simulated irradiance was calculated. The timestamps with front irradiance lower than 200 W/m^2 were excluded to reduce the influence of low light conditions. The daily fluctuations can be observed, and the ratio tends to decrease over time. When integrating the irradiance on sensors over all the non-snow days, the simulated irradiance is approximately 15% greater than the measured one.

This overestimation may arise due to fluctuating ground conditions that cannot be easily corrected using a single set of albedo parameters. A possible approach to solve this problem is to calculate albedos based on the measured rear irradiance for each timestamp. However, it faces significant challenges in implementing this method with the time-consuming ray-tracing simulation. What it used to mitigate the impact of this overestimation on power evaluation is to minimize the difference between simulated and measured irradiance averages across all days by using a set of decreased albedo parameters. With well-tuned albedo parameters, the difference between simulated and measured irradiance averages on sensors can be lowered to 0.87%. When applying this to the irradiance sampling on cells, the optical average bifacial gain of 9.7% can be evaluated across all non-snow days.

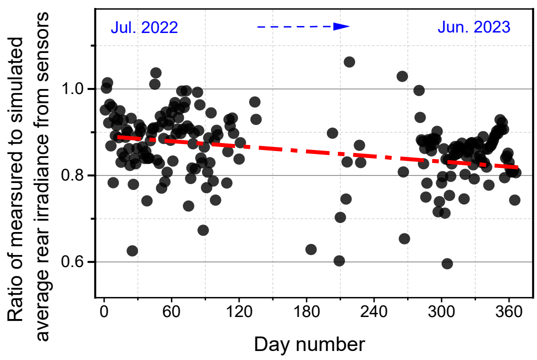

Figure 8 The ratio of measured to simulated daily averaged rear irradiance of days without snow on the ground. The red dash line is guide to eyes.

The hourly outputs with and without mismatch were simulated for all the non-snow days and then aggregated into days to calculate the ratio of measured to simulated daily energy outputs as shown in **Figure 9**. Clear sky filter is used to exclude the influence of low irradiance conditions. As **Figure 9** shows, the ratio is around 0.96 in July 2022 and then decreases to around 0.91 in June 2023. We attribute this reduction to the possible soiling and degradation effects on the system during the first year of installation. The annual degradation rate can be evaluated from the slope of the reduction as 5.6%. The value is very high compared to expected degradation of typical PV systems during the lifetime of the panels. However, this value shows only the first year of operation and it can be expected to slow down later.

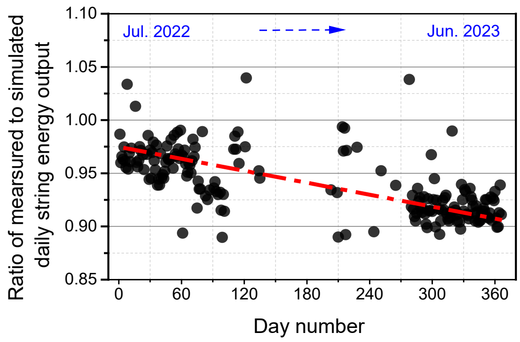

Figure 9 The ratio of measured to simulated daily averaged string power output of days without snow on the ground. The red dash line is guide to eyes.

It should be also noted that, as indicated in **Figure 8**, since the same albedo was used in all the simulations, the ratio of actual to simulated rear irradiance on the string will also decrease with time. This reduction should also contribute to the decrease in power output and cannot be easily distinguished from the electrical degradation unless hourly optimized albedo is used.

The dependence of mismatch loss on total irradiance was investigated. Two indicators of the standard deviation (STD, σ) and the mean absolute difference (MAD, Δ) were calculated as follows:

$$\sigma = \frac{1}{\bar{G}_{total}} \sqrt{\frac{\sum\left(G_{total,i} - \bar{G}_{total}\right)^2}{n}} \qquad (2)$$

$$\Delta = \frac{1}{n^2 \bar{G}_{total}} \sqrt{\frac{\sum_{i=1}^{n} \sum_{j=1}^{n} \left|G_{total,i} - G_{total,j}\right|}{n}} \qquad (3)$$

The relations between mismatch loss and irradiance variation STD and MAD are shown in **Figure 10**. The fitting proposed by Deline [8] is also drawn in **Figure 10** for comparison. For both indicators, the mismatch losses show a similar relationship between our case and Deline fitting in the low range of variation. However, when the variation is higher than 2%, the mismatch drops at a much steeper rate than the Deline fitting. This trend indicates that dependence could be case sensitive. The overall average power mismatch loss for all non-snow days was evaluated and found to be -0.37%.

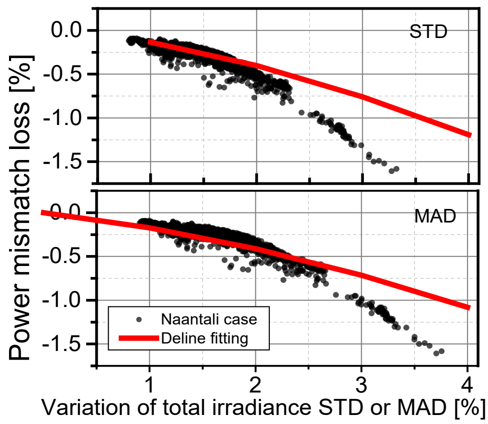

Figure 10 The dependence of power mismatch loss on the irradiance variation of STD or MAD of days without snow on the ground.

When analyzing the energy output across all non-snow days, the simulated energy output can be taken as the ideal energy output without any losses, which is 6.7 MWh for the 6.3 kWp target string, accounting for 87.5% of the total annual energy output. Compared to the measured energy output of 6.26 MWh, even considering the mismatch losses, there is still a gap of 0.41MWh, which accounts for about 6.1% of total energy production in non-snow days. Given that the annual degradation rate is 5.6%, the annual energy loss from degradation can be estimated to cover 2.8%-units by assuming a linear degradation. The remaining losses, approximately 3.3%-units, is then attributed to other factors.

(2) Days with snow

When the ground is covered by snow, the albedo is dramatically increased. **Figure** 11 shows the irradiance from back sensors for one snow week in March 2023. When the reference albedo for clear ground is used, the simulated average irradiance on sensors, which is shown as the red dot-line, is significantly lower than the measured values. For sunny days like 9 and 10 March, the rear irradiance is enhanced by almost twice at noon time.

The measured rear sensor irradiance can be well replicated with appropriately tuned parameters, as demonstrated by the black dot-line in **Figure** 11**.** The power output was then calculated and shown in **Figure** 12. The difference between the red and black lines indicates the increased power output resulting from enhanced rear irradiance due to snow. However, snow may stick to the front side of the PV modules and lower the power output, particularly in the morning of the 9th and 11th.

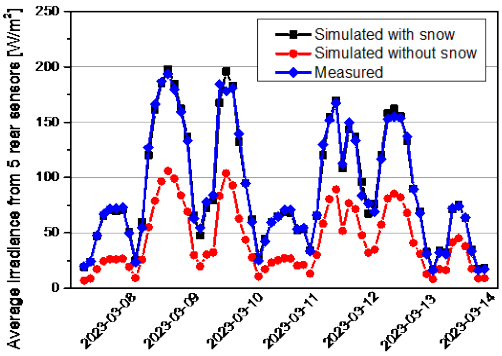

Figure 11 Measured and simulated hourly average irradiance of five rear sensors over one week with snow on the ground in March 2023.

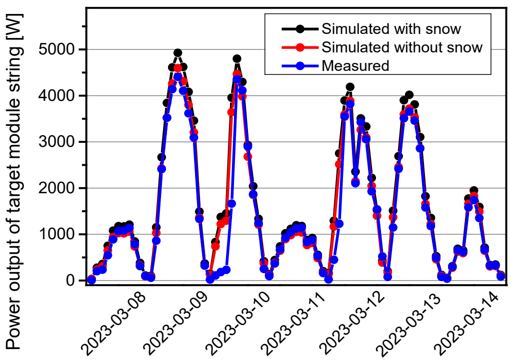

Figure 12 Measured and simulated hourly power output over one week with snow on the ground in March 2023.

Nevertheless, the problem remains that adjusting the albedo for every hour in all the snow days is unfeasible. The ground albedo changes gradually when the snow melts. Therefore, for the following simulations, we utilized a set of albedo parameters that produce an average irradiance on sensors which is comparable to the measured irradiance. With simulations for irradiance on cell and power output, the average bifacial gain during days with snow is 23.4%, which is 141% higher than for the days without snow. Assuming similar degradation and loss percentages as in non-snow days, we estimate that the snow coverage results in a loss of approximately 215 kWh, which accounts for 22.8% of the potential energy output during snow days.

(3) Energy analysis for the whole year

Here we consider both the days with and without snow to analyze the performance of the target string in one-year duration. The energy sources and losses are listed in Table 1. The energy output without mismatch is considered as the ideal energy output without any losses and is used as the reference to calculate the percentage of other components. Approximately 7% of the total energy output comes from the backside of the modules, with roughly 1% benefiting from snow. The mismatch loss accounts for around 0.5% of total energy production, which is a minor loss in our case, while the loss from snow coverage is relatively high at 2.8%. The findings suggest that, in our case, snow tends to have stronger negative effects than the positive one to the energy output. The proper estimation of snow-induced losses and the preventative measures for snow accumulation are important topics for the implementation of PV systems in high latitude areas.

Items			Energy [kWh]	Percentage [%]
Source	Front side		7105	92.97
	Rear side	Normal refelction	451	5.91
		Snow befeficial	86	1.13
Ideal total output			7642	100
Loss	Mismatch		37	0.48
	Snow coverage		215	2.81
	Degradation		214	2.80
	Others		257	3.36
Real total output			6920	90.55
Quasi-annual yield (for 343 days)			1098.45 hr	

Table 1 The Energy analysis of the target string in Naantali canopy system

3.2 Flat-Roof PV

1. Preliminary results

With the validated methodology, a preliminary simulation was performed for the Flat-Roof PV by using the meteorological data available from the Canopy-PV. As the system will be installed during autumn 2023, no DC power measurements are available for comparing the simulations, however preliminary inferences can be obtained for evaluating the benefits of having bifacial systems in this type of configurations.

a) Rear irradiance

For this evaluation, 3 modules were model in which was considered that the rear irradiance was the most affected. **Figure 13** shows the rear irradiance map at cell level for the 3 modules simulated where the edge effects are well defined. The 3rd module located at the end of the row (At the right) receives almost twice the light during some hours of the day compared to the modules that have other modules on both sides, therefore a higher mismatch effects are expected.

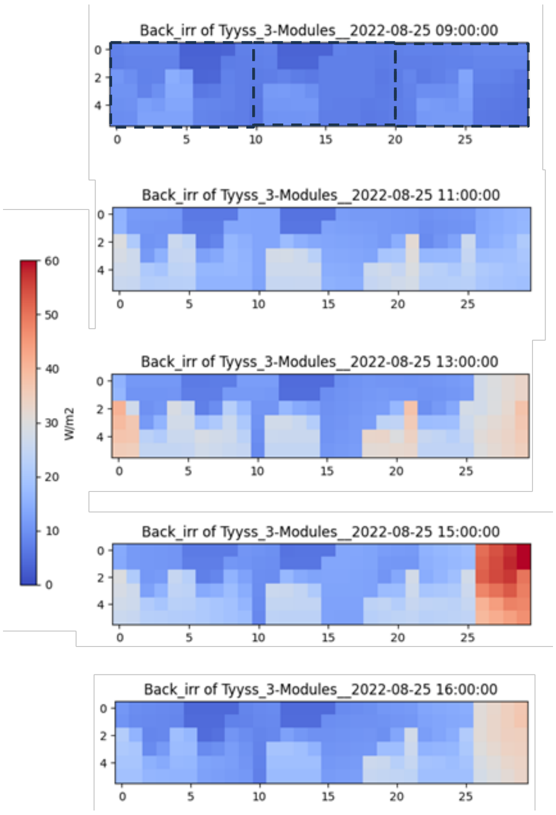

Figure 13: Rear irradiance map of the Flat-Roof array for 3 modules in a sunny day on 25 August 2022. The x- and y-axis indicate the number of cells. The perspective in the figure is from north to south. The three modules were chosen from the most representative array.

Optical bifacial gain from the Flat-Roof PV is shown in **Figure 14**. The estimated value during sunny days is around 2.5%, which is low due to the tilt angle and the clearance of less than 15 cm from the roof to the bottom edge of the modules. Average irradiance at the rear of the modules across the year was found to be 10 W/m^2 with maximum values up to 90 W/m^2.

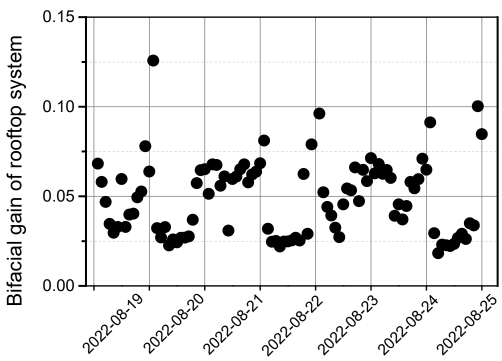

Figure 14: Hourly bifacial gain for the 3 modules, week from 19 to 25 in August 2022

b) Mismatch

The mismatch was calculated for this configuration as well **Figure 15**, the results show that a higher mismatch must be expected for this type of arrays, due to the racking systems and due to the amount of light limitations when the modules are in the middle of other modules compared to the ones at the end of the rows. At first glance seems that the mismatch is higher (estimated 4% for the whole year) for this configuration compared with the Canopy-PV, however a complete string of modules must be simulated, to make a proper comparison.

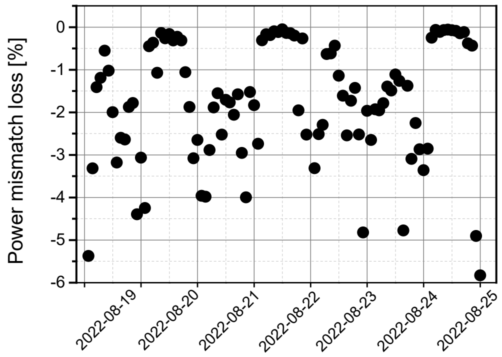

Figure 15. Hourly power mismatch for the Flat-Roof PV, from 19 to 25 in August 2022

c) Snow effects

Finally, a week of data was simulated with high albedo using the same snow conditions as presented for the Canopy-PV. Preliminary results show a 1.5 % increase in the power output of the systems when there is fresh now with an albedo value of 80%. It was found that the average irradiance was double at the rear of the modules reaching 11.5 W/m^2, under perfect snow conditions, i.e., fresh snow fully covering the roof. All these results to be evaluated once field data has been gathered.

4 CONCLUSIONS

Two BPV systems at high latitude sites were simulated using backward ray-tracing technique in combination with detailed 3D models and on-site meteorological data. An improved irradiance sampling method was developed to simulate an accurate irradiance map on each cell of the modules with high-speed asynchronous execution. This enabled detailed and accurate simulation of BPV system in a relatively short time. The goal was to evaluate their energy generation efficiency and losses, particularly in high-latitude locations with variable seasonal conditions, including snow.

The study validated the model's accuracy by comparing simulated and measured rear irradiance and DC power data. The power output of the Canopy-PV system was simulated over one year and compared with monitored data for an analysis of energy gain and loss. It showed that, with an annual bifacial gain of 7.5%, 7% of the total energy comes from the irradiance on the backside of the PV modules. The power mismatch loss due to irradiance variation on the backside was evaluated as 0.5%, which was not a major loss in our case. Snow, which is common during winter at high latitudes, had two opposing effects. On sunny days, it can double the irradiance on backside. The energy output resulted from this enhancement accounts for about 1% of the total energy. On the other hand, snow coverage on the front side could block the front irradiance and leads to a loss of 2.8% of the total energy. Therefore, appropriate snow clean-up measures might be important to further optimize the yield of PV systems in high latitude regions.

Preliminary results for the Flat-Roof PV array revealed that rear irradiance is significantly influenced by the module's position within the array, with edge modules receiving nearly twice the light. Bifacial gain during sunny days was estimated at approximately 2.5%, affected by factors such as the array's tilt angle and clearance. Additionally, mismatch calculations indicated a potential for higher mismatch in this configuration compared to the Canopy-PV system due to the presence of racking systems and shading from neighboring modules. Furthermore, simulations suggested a 1.7% increase in power output during snowy conditions, with rear irradiance peaking at 11.5 W/m^2 under ideal snow conditions.

Overall the study demonstrated the effectiveness of ray-tracing modeling for BPV systems, allowing for accurate predictions of rear irradiance, bifacial gain, power output, and mismatch. It highlighted the significance of variable ground conditions, snow effects, and module-level variations in BPV system performance. These findings emphasize the importance of considering these factors when designing and implementing BPV systems, especially in high-latitude regions with seasonal variations.

5 ACKNOWLEDGMENTS

The project has received funding from the European Union’s Horizon 2020 research and innovation program under Grant Agreements 957751 (RESPONSE) and 957769 (TIGON) as well as Finnish Cultural Foundation.

6 REFERENCES

[1] B. Marion et al., "A Practical Irradiance Model for Bifacial PV Modules," 2017 IEEE 44th Photovoltaic Specialist Conference (PVSC), Washington, DC, USA, 2017, pp. 1537-1542, doi: 10.1109/PVSC.2017.8366263

[2] Anoma, M., Jacob, D., Bourne, B.C., Scholl, J.A., Riley, D.M. and Hansen, C.W., 2017. View Factor Model and Validation for Bifacial PV and Diffuse Shade on Single-Axis Trackers. In 44th IEEE Photovoltaic Specialist Conference.

[3] Ward, Gregory J., Francis M. Rubinstein, Robert D. Clear, (1988). A Ray Tracing Solution for Diffuse Interreflection, Computer Graphics, Volume 22.

[4] Ward, G. J. (1994). The RADIANCE lighting simulation and rendering system. In 21st Annual Conference on Computer Graphics and Interactive Techniques (pp. 459–472). doi:10.1145/192161.192286

[5] Ayala Pelaez et al., (2020). Bifacial_radiance: a python package for modeling bifacial solar photovoltaic systems. Journal of Open-Source Software, 5(50), 1865, https://doi.org/10.21105/joss.01865

[6] Ranta S. et al., (2022). Bifacial PV Canopy System in High Latitude, Model Development and Validation with First Months of Monitoring Data. 8th World Conference on Photovoltaic Energy Conversion, doi: 10.4229/WCPEC-82022-4DO.5.6

[7] Nathaniel L. Jones & Christoph F. Reinhart (2019) Effects of real-time simulation feedback on design for visual comfort, Journal of Building Performance Simulation, 12:3, 343-361, DOI: 10.1080/19401493.2018.1449889

[8] Liang, Tian Shen, Pravettoni, Mauro, Deline, Christopher A., Stein, Joshua S., Kopecek, Radovan, Singh, Jai Prakash, Luo, Wei, Wang, Yan, Aberle, Armin G., and Khoo, Yong Shen. A Review of Crystalline Silicon Bifacial Photovoltaic Performance Characterization and Simulation. United States: N. p., 2018. doi:10.1039/C8EE02184H